Perutz, M. F. (1979) *Annu. Rev. Biochem. 48*, 327.
Perutz, M. F., Fersht, A. R., Simon, S. R., & Roberts, G. C. K. (1974a) *Biochemistry 13*, 2174.
Perutz, M. F., Heidner, E. J., Ladner, J. E., Beetlestone, J. G., Ho, C., & Slade, E. F. (1974b) *Biochemistry 13*, 2187.
Perutz, M. F., Sanders, J. K. M., Chenergy, D. H., Noble, R. W., Pennelly, R. R., Fung, L. W.-M., Ho, C., Giannini, I., Pörschke, D., & Winkler, H. (1978) *Biochemistry 17*, 3640.
Rots, M. J. F. (1982) Ph.D. Thesis, University of Groningen.
Rots, M. J. F., & Zandstra, P. J. (1982) *Mol. Phys. 46*, 1283.
Shelnutt, J. A. (1980) *International Conference on Raman Spectroscopy, 7th*, Ottawa, Aug 1980, Elsevier/North-Holland, New York.
Shelnutt, J. A., Rousseau, D. L., Friedman, J. M., & Simon, S. R. (1979) *Proc. Natl. Acad. Sci. U.S.A. 76*, 4409.
Smith, D. W., & Williams, R. J. P. (1970) *Struct. Bonding (Berlin) 7*, 1.
Vickery, L., Nozawa, T., & Sauer, K. (1976) *J. Am. Chem. Soc. 98*, 343.
Weissbluth, M. (1974) *Hemoglobin, Cooperativity and Electronic Properties*, Springer-Verlag, Berlin.
Zerner, M., Gouterman, M., & Kobayashi, H. (1966) *Theor. Chim. Acta 6*, 363.

Proton NMR Spectroscopy of Cytochrome *c*-554 from *Alcaligenes faecalis*†

Russell Timkovich* and Margaret S. Cork

ABSTRACT: Cytochrome *c*-554 from the bacterium *Alcaligenes faecalis* (ATCC 8750) is a respiratory electron-transport protein homologous to other members of the cytochrome *c* family. Its structure has been studied by ^{1}H NMR spectroscopy in both the ferric and ferrous states. The ferric spectrum is characterized by downfield hyperfine-shifted heme methyl resonances at 46.25, 43.60, 38.40, and 36.73 ppm (25 °C, pH 7.1). Chemical shifts of these resonances change with temperature opposite to expectations derived from Curie's law. The pH behavior of the hyperfine-shifted resonances titrates with a p*K* of 6.3 that has been interpreted as due to ionization of a heme propionate. In the ferrous state, heme methyl, meso, and thioether bridge resonances have been observed and assigned. All aromatic proteins have been assigned according to the side chain of origin, and the structural environment about the sole tryptophan residue has been examined. The electron-transfer rate between ferric and ferrous forms has been estimated to be on the order of 3×10^8 M^{-1} s^{-1}, which is the largest such self-exchange rate yet observed for a cytochrome.

Comparison of cytochrome structures and properties contributes to understanding the function of these ubiquitous electron-transport proteins. Cytochromes *c* play such an integral role in respiration that they are found widely distributed not only in eukaryotic cells but also in almost all prokaryotic cells. Proton NMR spectroscopy is a useful technique for making structural comparisons among cytochromes *c*. It is made more powerful by the three-dimensional data available from X-ray crystallography on a limited number of archetype cytochromes and the growing number of NMR assignments that have been achieved.

Recently the isolation and partial characterization of a low molecular weight cytochrome *c* were reported for the bacterium *Alcaligenes faecalis* (ATCC 8750) (Timkovich et al., 1982). On the basis of its visible spectrum in the reduced state, it has been termed cytochrome *c*-554. It functions in the electron-transport chain of *Alcaligenes*, donating electrons to a soluble nitrite reductase during denitrification and presumably to a membrane cytochrome oxidase during aerobic respiration. It has approximately 86 amino acids, and its amino acid composition is similar to that of cytochrome *c*-551 from *Pseudomonas aeruginosa*. Cytochromes with this relatively low molecular weight appear to constitute a subclassification of the general cytochrome *c* family (Dickerson et al., 1976). *Pseudomonas* cytochrome *c*-551 has been studied by X-ray crystallography (Almassy & Dickerson, 1978) and by proton NMR (Keller, R. M., et al., 1976; Moore et al., 1977; Chao et al., 1979). Potentially homologous photosynthetic cytochromes *c*-553 from cyanobacteria have also recently been the subject of an NMR investigation (Ulrich et al., 1982). Structural results have revealed interesting differences between these low molecular weight cytochromes and the larger eukaryotic cytochrome *c* that include different chirality about the axial sulfur ligand (Senn et al., 1980) and a different distribution of spin density in the oxidized form (Keller & Wuthrich, 1978a,b). It is plausible that further differences in the precise structure exist among the many variants of cytochrome*c*.

Proton NMR data are presented here for cytochrome *c*-554 from *Alcaligenes*. The results broaden the basis for comparisons of cytochrome structure and contribute assignment data for critical elements of the protein. Features of the *c*-554 spectra are unique and have not been previously observed for a member of the cytochrome *c* family.

Materials and Methods

Alcaligenes faecalis (ATCC 8750) was cultured and the cytochrome *c*-554 purified as described previously (Timkovich et al., 1982). The spectroscopic purity ratio of the absorbance at 409 nm to that at 280 nm was greater than 5.2 for all

† From the Department of Chemistry, Illinois Institute of Technology, Chicago, Illinois 60616. *Received April 8, 1983.* Financial support was provided by Grant GM-23869 from the National Institutes of Health. The NMR facility was supported by a grant from the NIGMS Shared Instrumentation Program of the National Institutes of Health (GM-26071-02S1).

0006-2960/84/0423-0851$01.50/0

samples used in the present study. Three independent batches of cytochrome *c*-554 were prepared and handled separately. All gave indistinguishable NMR spectra.

Samples for NMR spectroscopy were dialyzed vs. 50 mM ammonium bicarbonate, pH 7.8, lyophilized, and then redissolved in 99.8% deuterium oxide buffered to the appropriate pH. Values of pH labeled as pH* were determined by using a glass combination microelectrode calibrated against ^1H standards and are reported as the uncorrected, direct reading. For pH titrations, adjustments were made with solutions of ^2HCl or NaO^2H. The standard buffer for all samples was 10 mM in phosphate (Na/Na) and 100 mM in NaCl. Reduced cytochrome was prepared by the addition of a minimal excess of solid sodium dithionite. For long-term data acquisition on some samples, reduced protein was sealed in glass 5-mm NMR tubes after alternate cycles of vacuum evacuation and argon flushing to prevent slow autoxidation of the cytochrome by air.

Samples containing mixtures of ferro- and ferricytochrome were prepared by splitting a stock solution into two appropriate volumes, reducing one portion with a minimum amount of solid sodium dithionite, allowing the reduced portion to stand for several hours with occasional shaking in air to eliminate excess dithionite, and then remixing the portions. The fractional amount of reduced cytochrome was checked by visible spectroscopy before and after data collection by pipetting the sample into 1-mm path-length cells and monitoring the absorbance at the reduced α band vs. an isosbestic point at 540 nm. In our hands, we could not accurately check the fraction of oxidized cytochrome in the presence of a large excess ($\geq$90%) of reduced cytochrome, because the relative contribution of the broad oxidized absorption is small compared to the intense, sharp reduced α band. In cases involving low fractions of oxidized cytochrome, there is uncertainty about the actual fraction, because it is likely that the reduced portion underwent some autoxidation during the waiting before mixing. Pilot experiments involving just absorption spectroscopy indicated that a nominal 1% oxidized sample prepared as described could become as high as 10% oxidized.

^1H NMR spectra were obtained on a Nicolet spectrometer operating at 300 MHz in the Fourier-transform mode and equipped with a variable-temperature proton probe. Chemical shifts are reported in parts per million from internal sodium 4,4-dimethyl-4-silapentane-1-sulfonate (DSS). Spectra obtained without DSS, in which residual H^2HO was used as a shift standard, were indistinguishable from spectra with DSS. Peak intensities were determined by the Nicolet software integration routine or by cutting and weighing plotted spectra. The well-resolved meso protons in ferrocytochrome *c*-554 were used as an internal standard to calibrate the intensity of a single proton. Sample concentrations ranged from 0.2 mM for routine spectra to 3 mM for nuclear Overhauser enhancement measurements. No protein concentration spectral effects were observed.

Spectra to be shown for the aromatic region of ferrocytochrome *c*-554 were resolution enhanced by applying a double-exponential apodization function to the free induction decay before transformation. Spin–lattice relaxation times were measured by an inversion–recovery pulse sequence using phase-shifted pulses to eliminate certain potential artifacts (Freeman et al., 1980). Experiments on steady-state nuclear Overhauser enhancements (Keller & Wuthrich, 1978a), *J*-modulated, spin-decoupling difference spectroscopy (Campbell & Dobson, 1975), and truncated-driven nuclear Overhauser enhancement (Dubs et al., 1979) have been previously described. Data from pH titration studies were analyzed by a nonlinear least-squares algorithm (Timkovich & Cork, 1982).

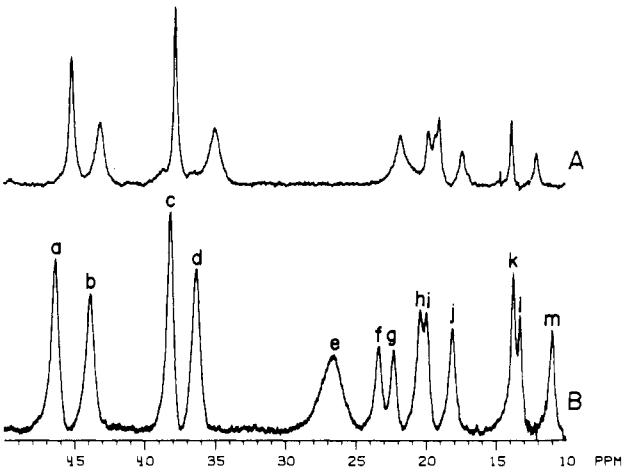

FIGURE 1: Downfield region of the ^1H NMR spectrum of *Alcaligenes faecalis* ferricytochrome *c*-554. Protein concentration was 1 mM in 99.8% deuterium oxide buffered with 10 mM phosphate plus 100 mM NaCl at pH* 7.6. (A) Temperature 13 °C; (B) temperature 28 °C.

Optical spectra were obtained on a Perkin-Elmer Lambda 5 spectrophotometer in standard 1-cm cuvettes in both H_2O and ^2H_2O.

Results

Optical Spectroscopy of Cytochrome c-554. The optical spectrum of ferrocytochrome c-554 had maxima at 554, 523, and 418 nm. These wavelengths are typical for *c*-type cytochromes except for the 4-nm red shift of the α band. The reduced pyridine hemochromogen possessed an α-band maximum at 550 nm. Thus, some aspect of the protein environment is responsible for the 4-nm shift in native protein. Ferricytochrome *c*-554 possessed bands at 410, 525, and 695 nm. The 695-nm band was unaffected by lyophilization and was also observed when the solvent was 99.8% deuterium oxide. The 695-nm band is an indicator of methionine ligation in cytochromes *c* [see Dickerson & Timkovich (1975) and references cited therein]. Optical spectra were obtained for the ferricytochrome in the presence of potential exogenous ligands. In the presence of 100 mM potassium cyanide, the ferric visible spectrum showed loss of the 695-nm band and a shift of the remaining bands to 414 and 529 nm. These are highly comparable optical effects to the case of mammalian cytochrome *c* in the presence of cyanide and indicate displacement of the sixth ligand methionyl sulfur by cyanide [see Dickerson & Timkovich (1975) and references cited therein]. The addition of 100 mM sodium fluoride or sodium azide did not affect the optical spectrum of the native ferricytochrome *c*-554. Fluoride is not known to bind to any cytochrome *c* in its native conformation, and azide binds only very weakly to mammalian cytochromes *c* (Gupta & Redfield, 1970) and not at all to many bacterial cytochromes (R. Timkovich, unpublished results).

Ferricytochrome c-554: Spectrum and Temperature Dependence. The spectra of the ferric form of *Alcaligenes c*-554 at two different temperatures are shown in Figure 1. As expected for this paramagnetic protein, numerous hyperfine-shifted resonances are apparent downfield of 10 ppm. It will be important to note that no additional resonances were observed in the spectral range up to 150 ppm. Data for the resolved resonances of ferricytochrome are summarized in Table I. The structure of the heme prosthetic group is shown in Figure 2. In analogy with other cytochromes *c*, the four

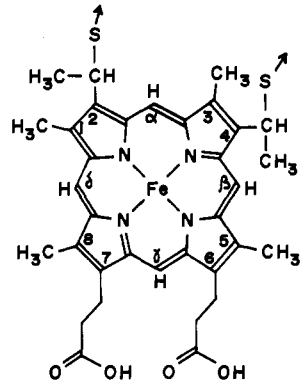

FIGURE 2: Structure and nomenclature of heme *c*. The substituent positions of the pyrrole rings are numbered 1–8, and the four meso protons are labeled α–δ. The arrows from the sulfur atoms indicate attachment to the remaining portion of the cysteine residues. In this orientation, the axial histidine is below, and the axial methionine above, the plane of the ring.

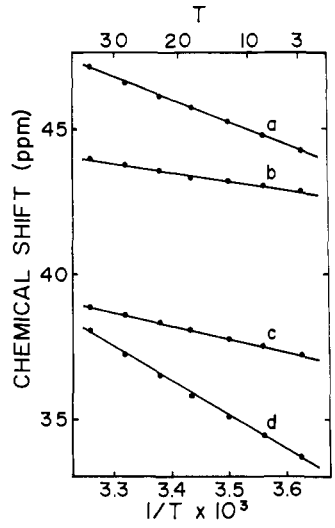

FIGURE 3: Temperature dependence of select hyperfine-shifted resonances in ferricytochrome *c*-554. The resonances shown are the heme methyls designated a–d in Figure 1 and Table I. Plots of chemical shift vs. $1/T$ in degrees kelvin were linear within experimental error, and data for all resolved resonances are summarized in Table I as slopes and intercepts. The upper scale in degrees centigrade is shown to clarify that shifts increase with increasing temperature.

heme ring methyl groups are expected to show large downfield hyperfine shifts mainly due to the contact shift mechanism (Shulman et al., 1971). The observed methyl resonances designated a–d have been assigned to the heme ring methyl groups.

The ferricytochrome spectrum had a marked temperature dependence as shown in Figure 1. The heme methyl resonances, especially b and d, show dramatic line broadening at lower temperature. Hyperfine chemical shifts also show a strong dependence on temperature. The observed variation with temperature is plotted in Figure 3 for select resonances, and the effect for other resolved resonances is summarized in Table I. The most striking observation is that the direction of change with respect to temperature is opposite from that predicted by a Curie's law dependence.

Spin–Lattice Relaxation in Ferricytochrome c-554. Values for the spin–lattice (T_1) relaxation times for resolved resonances at 30 °C are summarized in Table I. Quantitative interpretation would require more extensive temperature and field strength data than currently available. However, comparison of the current data with T_1 data reported for horse heart cytochrome *c* (Redfield & Gupta, 1971) does reveal that

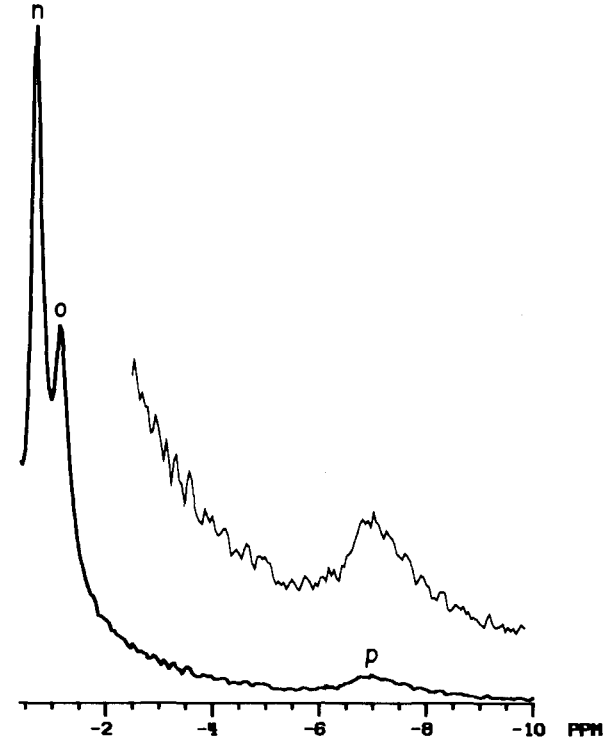

FIGURE 4: Upfield region of the ^{1}H NMR spectrum of ferricytochrome *c*-554. The spectrum shown is for 25 °C and pH* 7.5. In contrast to the downfield region, this upfield region does not exhibit drastic changes with temperature or pH. Chemical shift behavior is summarized in Table I. No further resonances were observed upfield of resonance p in spectra examined to −140 ppm.

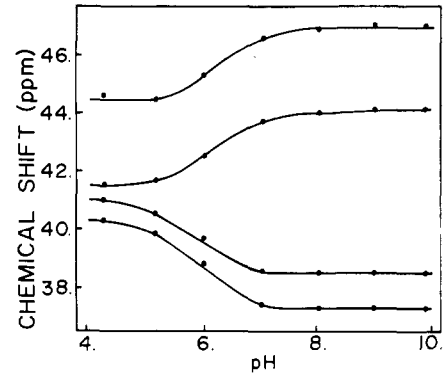

FIGURE 5: Effect of pH on the hyperfine-shifted heme methyl resonances of *Alcaligenes* ferricytochrome *c*-554. Temperature was 30 °C. Effects for other resolved resonances are given in Table I.

relaxation in *c*-554 is significantly faster than in horse heart cytochrome *c*.

Effects of pH on Ferricytochrome c-554. At pH* values approaching the extremes of 4 and 10, the intensities of the hyperfine-shifted resonances decreased. The pK of the acidic transition was estimated to be at least 1 unit below 4. Insufficient data preclude a more quantitative determination. The high-pH intensity change titrated with an apparent pK of 9.8. These effects were attributed to the well-known ligand-exchange reactions of cytochrome *c* (Dickerson & Timkovich, 1975) in which the histidine ligand is displaced at low pH and the methionine ligand at high pH.

An additional pH effect near neutrality was observed for *c*-554 in which hyperfine resonances showed changes in the chemical shift, but not intensity. Figure 5 displays the chemical-shift dependency for select resonances, and Table I summarizes data for all resolved resonances. Titration data for resonances showing a total shift of greater than 0.2 ppm

Table I: Proton NMR Data for *Alcaligenes* Ferricytochrome *c*-554

label[a]	chemical shift (ppm)[b]	peak area[c]	temp coefficients[d] a	temp coefficients[d] $b \times 10^{-3}$	pH* sensitivity[e] (ppm)	T_1[f] (ms)
a	46.25	3	72.2	−7.7	10.5	36
b	43.60	3	52.3	−2.6	+2.6	30
c	38.40	3 + 1[h]	53.9	−4.6	−2.5	36
d	36.73	3	76.0	−11.7	−2.0	33
e	26.70	3[i]	157.0	−38.7	+1.4	1
f	23.52	1	63.2	−11.8	+0.05	33
g	22.05	1	73.8	−15.4	+5.5	36
h, i	20.43[g]	2	52.3	−9.5	−3.7, +0.7[k]	16
j	18.22	1	36.2	−5.4	−0.5	5
k	13.80	1	10.7	+0.9	−0.3	17
l	13.39	1	44.1	−9.2	−0.3	17
m	11.09	1	52.4	−12.3	−0.4	7
n	−0.70	3[j]	−0.70	0	−0.2	
o	−1.10	3[j]	−1.10	0	+0.3	
p	−6.75	1	−6.75	0	−1.5	1

[a] Peak labels correspond to those used in Figure 1. [b] From internal DSS at 25 °C, pH* 7.1. [c] Protons per mole of cytochrome. [d] Temperature data as depicted in Figure 2 for select resonances were fit to an equation linear in reciprocal temperature in kelvin: $\omega_T = a + b/T$ where ω_T was the observed shift at temperature T. The parameters a and b represent the best-fit least-squares result. For peaks downfield of DSS, a positive sign for b would indicate that the resonance position followed Curie's law behavior. Negative values indicate some other mechanism is reponsible for the temperature effect. Since few of the observed resonances followed Curie's law, there is no theoretical justification for assuming linearity with $1/T$. However, empirically the data were linear with respect to $1/T$ over the actual temperature range studied, 275–319 K. In principle, parameter a would represent the chemical shift extrapolated to infinite temperature. However, the temperature range studied was small, and the mechanism of the shifts is uncertain. The reported coefficients should only be taken as a convenient empirical method of summarizing observed shifts. [e] The pH sensitivity is for the transition that occurs with pK = 6.3. Values represent the change in chemical shift upon going from pH* 4 to pH* 9. A positive value indicates a high shift at pH* 9. [f] Measured at 30 °C. [g] Above 30 °C, this peak resolves into two peaks with a splitting of 132 Hz. These peaks represent distinct spin systems as evidenced by the pH dependence. See also, footnote *k*. [h] This peak consistently integrated to greater than 3.7 protons per mol of cytochrome (actual average = 3.9). It is interpreted as a methyl group and an unresolved single proton resonance. [i] Integration was most difficult for this peak because of its great peak width and low signal to noise ratio in some spectra. The actual average was 2.8 protons, and the observed range of values was from 2.5 to 3.2 protons. [j] Estimates only, because of incomplete resolution. [k] At pH* 4, this nonresolved peak splits into two single proton peaks with chemical shifts of +24.4 and +20.0 ppm.

were fit by a one-proton titration curve, yielding an average transition pK of 6.3 ± 0.2.

A definitive assignment of the group undergoing titration with a pK of 6.3 cannot be made at this time. Serious consideration must be given to the hypothesis (Keller, R., et al., 1976; Chao et al., 1979; Moore et al., 1980) that the group is one of the propionic side chains of the heme. A transition with a pK near 6 has not been observed by NMR for eukaryotic cytochromes. However, many prokaryotic cytochromes seem to share this transition in common. The reported cytochrome, organism, and observed pK are the following: cytochrome c_2 from *Rhodospirillum rubrum* at 6.25 (Smith, 1979), cytochrome *c'* from *R. rubrum* at 5.8 (Emptage et al., 1981), cytochrome *c*-551 from *Pseudomonas aeruginosa* at 5.8 (Chao et al., 1979), cytochrome cd_1 from *Paracoccus denitrificans* at 5.8 (Timokvich & Cork, 1982), and cytochrome *c*-550 from *P. denitrificans* at 6.2 (R. Timkovich, unpublished results). Certain chemical modifications near the

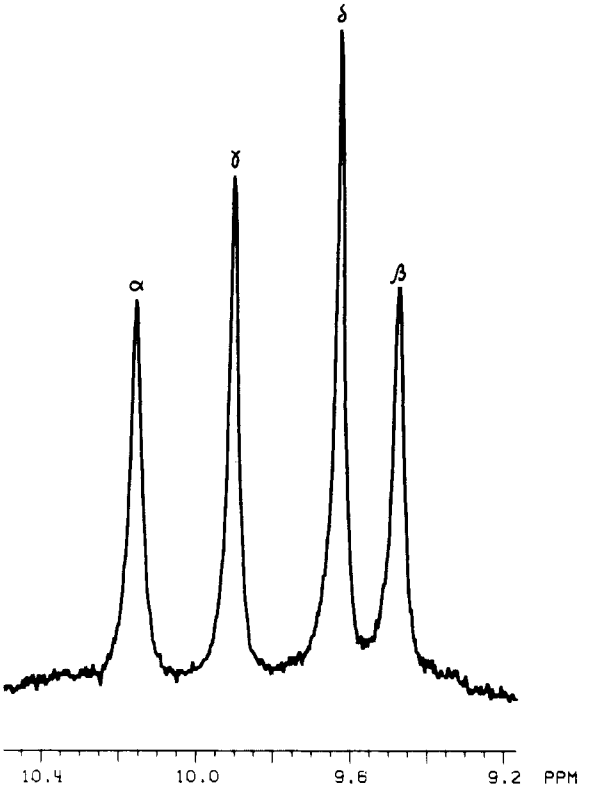

FIGURE 6: Spectrum of the heme meso protons in *Alcaligenes* ferrocytochrome *c*-554 at 40 °C, pH* 8. Resonances are labeled according to the assignments discussed in the text and Table II.

site of the propionates in eukaryotic cytochrome *c* do lead to derivatives that show transition pKs in their visible spectra with pKs near 6 (Timkovich, 1980). These examples cover such a diverse range of sequences and structures that the only conserved, ionizable group in common appears to be the heme propionate. It may be that the hydrogen-bond network around the propionates in eukaryotic cytochrome *c* normally precludes ionization, unless the network is disrupted by chemical modification. In the bacterial cytochromes, the hydrogen bonds may be sufficiently relaxed that the propionate ionization is readily observed. The mechanism for the chemical-shift differences may be minor electronic and orientation differences for the heme in the heme pocket.

Cyanide Complex of Ferricytochrome c-554. In the presence of 100 mM cyanide at pH* 7 and 34 °C, the proton spectrum of ferricytochrome *c*-554 shows four hyperfine-shifted resonances at 25.2, 19.2, 16.5, and 10.8 ppm. The spectrum resembles that of eukaryotic cytochrome *c* (Wuthrich, 1969) where corresponding resonances were observed at 22.9, 21.1, 16.0, and 11.4 ppm. As is also the case in eukaryotic cytochrome *c*, other hyperfine-shifted resonances from the native ferric protein have become difficult to detect.

Ferrocytochrome c-554 Spectrum and Assignments. The downfield region of the proton spectrum of deuterium-exchanged ferrocytochrome *c*-554 is shown in Figure 6. No additional peaks were observed further downfield, consistent with the sample being diamagnetic. The four clearly resolved resonances are unambiguously assigned to heme meso protons based on spectral correlations with model compounds and other heme proteins (La Mar & Walker-Jensen, 1979; Ulrich et al., 1982).

The upfield region of the ferrocytochrome spectrum is shown in Figure 7A. The prominent three-proton resonance at −2.98 ppm may be assigned with confidence to the heme sixth ligand methionyl methyl. In all ferrocytochromes *c* studied to date,

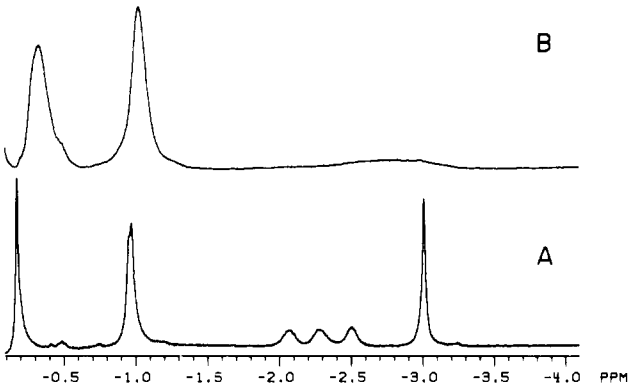

FIGURE 7: ^{1}H NMR spectra of the upfield region of *Alcaligenes* ferrocytochrome *c*-554 at 40 °C and pH* 8: (A) fully reduced *c*-554; (B) reduced *c*-554 containing a nominal 1% oxidized cytochrome. Independent, duplicate experiments indicated that the actual concentration of the oxidized form may have been as high as 10% because of autoxidation of the ferrocytochrome due to manipulations before data acquisition and the length of time for data acquisition.

this methyl group has been observed within a range of −2.8 to −3.3 ppm [for example, see Ulrich et al. (1982)]. The consistency of its chemical shift is to be expected, since the shift is dominated by the heme ring current. The one-proton resonances at −2.09, −2.29, and −2.49 ppm may be assigned to ligand methionyl C_β and C_δ protons, again on the basis of correlation to other ferrocytochromes (Senn et al., 1980). The three-proton resonances at −1.0 and −0.2 ppm resemble features in the spectra of ferrocytochromes *c*-553 from algae (Ulrich et al., 1982) and thus suggest structural homology with these proteins. Specific assignments in any cytochrome have not been accomplished.

Figure 7B shows the effect of adding a small fraction of ferricytochrome to a sample predominantly containing ferrocytochrome. The sample was prepared with a nominal ratio of 1% oxidized to 99% reduced, but it could have been as much as 10% oxidized due to autoxidation before the spectrum was obtained or during the time course of data accumulation. It is clear that the resonance at −2.98 ppm has been drastically affected by the presence of oxidized cytochrome. The resonances at −0.2 and −1.0 ppm have also been broadened and have undergone shifts of 0.28 and 0.12 ppm, respectively. Additional features not shown include collapse of the meso protons to a single unresolved peak at 9.9 ppm and loss of fine detail in the aromatic region. This spectrum of mixed oxidation states is not the simple superposition of individual ferri and ferro spectra. Such behavior has been taken to indicate rapid chemical exchange between the two forms due to rapid electron transfer. For example, in the case of *Pseudomonas* cytochrome *c*-551, mixed-state spectra have been used to measure an electron-transfer exchange rate of 10^7 M^{-1} s^{-1} (Keller, R. M., et al., 1976). Assuming that resonance e in ferricytochrome *c*-554 is the methionyl methyl (see Discussion concerning this hypothesis), then crude estimates based upon coalescence of lines in chemical-exchanging systems (Pople et al., 1959) estimate that the bimolecular electron-transfer rate constant must be 10^8 M^{-1} s^{-1} or greater. The −2.98 ppm resonance is not fully satisfactory for estimating exchange rates for several reasons. There is uncertainty that resonance e has been correctly assigned. In our hands, there is uncertainty about the exact concentration of ferricytochrome in a predominantly ferrocytochrome sample. The broad remaining feature in Figure 7B around −3 ppm may or may not be the previous −2.98 ppm resonance. The feature could be a coalescence of the previous resonances at −2.09, −2.29, and −2.49 ppm or some combination thereof.

Table II: Proton NMR Assignments[a] for *Alcaligenes* Ferrocytochrome *c*-554

ligand Met	S-CH_3, −2.98; methylene protons, −2.49, −2.29, −2.09
heme meso	α, 10.17; β, 9.48; γ, 9.90; δ, 9.63
heme methyls	1-methyl, >4 or 3.72; 3-methyl, 3.82; 5-methyl, 3.41; 8-methyl, 3.72 or >4
thioether bridges	2-methyl, 2.28; 2-methine, 5.80; 4-methyl, 2.44; 4-methine, 6.20
tyrosine	C2,6 or C3,5, 6.74 (6.8);[b] C3,5 or C2,6, 6.10 (6.8)
tyrosine	C2,6 or C3,5, 6.65 (7.8); C3,5 or C2,6, 5.95 (7.8)
tryptophan	C2, 7.79; C4 or C7, 7.75; C5 or C6, 7.15; C6 or C5, 6.91; C7 or C4, 5.95
phenylalanine (?)	6.6, 6.1, 5.55

[a] Chemical shifts in ppm from DSS at 40 °C. Nomenclature for heme protons is given in Figure 2. Nomenclature for aromatic amino acid protons is according to IUPAC-IUB conventions (IUPAC-IUB Commission on Biochemical Nomenclature, 1973). [b] Numbers in parentheses are the observed coupling constants in hertz.

The crude estimate was checked in another fashion. A mixed sample was prepared containing 96% oxidized cytochrome and 4% reduced cytochrome. The relative proportions could be confirmed in this case by visible spectrophotometry, because the reduced α band at 554 nm is a measurable shoulder on the broader absorption band of the oxidized form at 524 nm. The spectrum of the mixed sample was not the superposition of each pure oxidation-state spectrum. The mixed spectrum was of poor quality with low a signal to noise ratio. The extreme downfield hyperfine-shifted methyl resonances associated with the paramagnetic oxidized state were difficult to detect accurately but appeared to be shifted slightly upfield and broadened. The furthest downfield methyl resonance, at 46.3 ppm with a line width of 115 Hz in the pure oxidized form, appeared centered at 44.7 ppm with an approximate line width of 315 Hz. This shift enables a better estimate to be made of the oxidized–reduced exchange rate. For the case of fast exchange and exchange narrowing [see eq 9 and 10 of Mclaughlin & Leigh (1973)], the average chemical shift is given by

$$\omega = \omega_A f_A + \omega_B f_B \quad (1)$$

with a transverse relaxation time given by

$$1/T_2 = f_A/T_{2A} + f_B/T_{2B} + f_A f_B \tau_{AB} \Delta\omega_{AB}^2 \quad (2)$$

where ω_A and ω_B are the chemical shifts and T_{2A} and T_{2B} are the transverse relaxation times in the pure A and B states, respectively, f_A and f_B are the respective fractional populations, $\Delta\omega_{AB}$ is the chemical-shift difference between ω_A and ω_B, and τ_{AB} is defined by

$$\tau_{AB} = \frac{\tau_A \tau_B}{\tau_A + \tau_B} \approx \tau_B$$

for $\tau_A > \tau_B$ with τ_A and τ_B being the lifetimes in the A and B states, respectively. In the present case, the A state is identified with the oxidized form and the B state with the reduced. In the pure reduced state, heme methyls are found at circa 4 ppm with line widths of 30 Hz or less (from Table II and Figure 8). The upfield shift of circa 1.6 ppm in the 96% oxidized sample approximately matches the prediction of eq 1 and suggests that eq 2 may be used to calculate exchange rate data. This is an assumption, because it is not possible to directly observe heme methyls in the 4 ppm region in the mixed state. Substitution of the pure-state shifts and transverse relaxation times (computed from the observed line width) with the known fractions and the observed T_2 of the

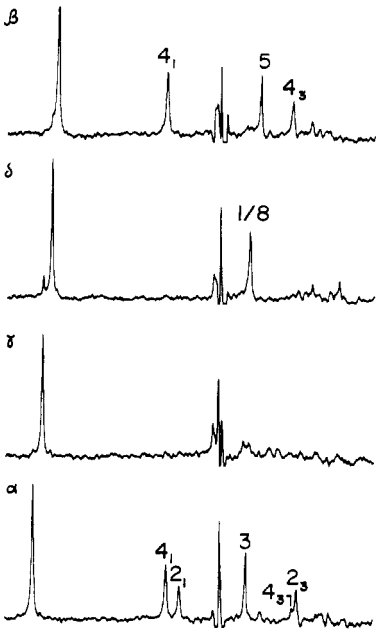

FIGURE 8: Nuclear Overhauser enhancements produced by preirradiation of the heme meso protons in *Alcaligenes* ferrocytochrome *c*-554. Preirradiation of the meso proton at 9.48 ppm (labeled β) produced an enhancement at 6.20 (labeled 4_1), 3.41 (5), and 2.44 ppm (4_3). Preirradiation of the meso proton at 9.63 (δ) ppm produced an enhancement at 3.72 ppm (1/8). Preirradiation at 9.90 ppm (γ) did not produce a significant enhancement anywhere. Preirradiation at 10.17 ppm (α) produced multiple enhancements at 6.20 (4_1), 5.80 (2_1), 3.82 (3), 2.28 (2_3), and weakly at 2.44 ppm (4_3). The resonance designations above correspond to assignments discussed in the text. All cases shown are difference spectra between a spectrum obtained with preirradiation at the stated position minus a control with irradiation at a dummy vacant position.

mixed sample allowed calculations of τ_{AB}. From this, a bimolecular electron rate transfer rate constant of 5×10^8 M^{-1} s^{-1} is predicted. Because of the quality of the data and the assumptions made in both approaches, this rate should be considered an estimate only. Additional mixed-state samples were prepared in which the percentage of oxidized material was varied from 20% to 97% and checked by visible spectrophotometry. Resonances were sought that systematically mapped from one chemical shift in one oxidation state to a different shift in the other. Because of incomplete resolution and the paramagnetic line widths, only two other systems could be followed with any confidence. Ferrocytochrome resonances at −1.0 and 7.79 ppm systematically shifted to −1.10 and 8.10 ppm in the manner predicted by eq 1. Line widths appeared to be dominated by T_2 for the paramagnetic oxidized form, that is, no additional line broadening due to exchange was observed. However, the chemical shift differences between the two pure forms are small, and the third term of eq 2 becomes negligible.

Negative nuclear Overhauser enhancements (NOE's) were observed between the ferrocytochrome meso protons and other heme protons. The theoretical and structural analyses of these enhancements have been explained in a series of papers (Keller & Wutrich, 1978a,b; Keller et al., 1980; Ulrich et al., 1982). The present discussion will focus on equivalent experiments but new results for *Alcaligenes c*-554. Spectra demonstrating the enhancements are shown in Figure 8.

Irradiation of the meso proton at 9.91 ppm did not produce a significant NOE in the aromatic or aliphatic regions. This leads to the assignment of the 9.91 ppm resonance to the meso proton γ. Irradiation of the three remaining meso protons each produced an NOE in the aliphatic region between 3 and 4.5 ppm which is the expected location for ferrous heme ring methyl groups. However, only irradiation at 10.17 and 9.48 ppm produced an NOE in the aromatic region where heme bridge thioether methine protons are expected. Therefore, the meso proton at 9.63 ppm is assigned to the meso proton δ. This experiment should produce two heme ring methyl NOE's corresponding to ring methyls at positions 1 and 8. Only one has been observed. The missing methyl is believed to be obscured by the artifact at 4.8 ppm that comes from residual HDO and is always present in our experiments.

Irradiation of the meso proton at 9.48 ppm produced an enhancement of a thioether bridge methine at 6.20 ppm, a ring methyl at 3.41 ppm, and a bridge methyl at 2.44 ppm. Therefore, the meso proton is either β or α. Irradiation at 10.17 ppm produced enhancements again at 6.20 ppm, weakly at 2.44 ppm, and at 5.80 and 2.28 ppm. The latter correspond to another thioether bridge methine and methyl, respectively. Truncated-driven NOE experiments (Dubs et al., 1979) indicated that the buildup rates of the enhancements at 6.20 and 5.80 ppm were comparable and faster than the buildup rate for the 2.28 ppm resonance which in turn was faster than that for the 2.44 ppm resonance. The only meso proton which is in a position to simultaneously produce enhancements of two bridge methines is the α meso proton. This assigns the 10.17 ppm meso proton as α. The other meso proton at 9.48 ppm which produced an enhancement of only one bridge group must be β, and the corresponding enhanced bridge resonances at 6.20 and 2.44 ppm must be at the 4 heme ring substituent position. Then the methine and methyl at 5.80 and 2.28 ppm are assigned to the 2-position. The fact that both bridge methine protons show large enhancements upon irradiation of the α meso proton indicates that groups are oriented so as to place both methine protons approximately equidistant from the α meso proton. This configuration is different from the situation in mammalian cytochrome *c* (Keller & Wuthrich, 1978b) or *Pseudomonas* cytochrome *c*-551 (Senn et al., 1980) where the 4-position bridge methine is directed away from the α meso proton and toward the β meso proton. In *Alcaligenes c*-554, rotation of both bridge groups would be necessary to make the methine protons approximately equidistant from the α meso proton.

The assignment of the α and β meso protons leads to the assignment of the enhanced heme methyl at 3.82 ppm to substituent position 3 and the heme methyl at 3.41 ppm to position 5. Irradiation of the bridge methyl at 2.44 ppm produced a weak enhancement of the 3-position heme methyl consistent with current assignments. Irradiation of the 2-position bridge methyl gave a complex difference spectrum with multiple peaks, none of which corresponded to any previously resolved heme methyl resonance. At 2.28 ppm, the spectrum of ferrocytochrome *c*-554 is extremely crowded, so that NOE irradiation is quite nonselective. It may be that multiple enhancements are obscuring any heme methyl signals. Alternatively, there may be an enhancement to the ring methyl believed to have a chemical shift greater than 4.2 ppm, and this is obscured by the HDO artifact.

Homonuclear decoupling experiments confirmed that the spin systems at 6.20 and 2.44 ppm were indeed coupled. For reasons that are not clear, spin coupling was not conclusively observed between the 2-position methine and the methyl at 5.80 and 2.28 ppm. No coupling was observed between those spin systems and any other portion of the spectrum.

The aromatic region of ferrocytochrome *c*-554 is shown in Figure 9. The thioether bridge methine protons are evident as unresolved multiplets at 6.20 and 5.80 ppm. From the

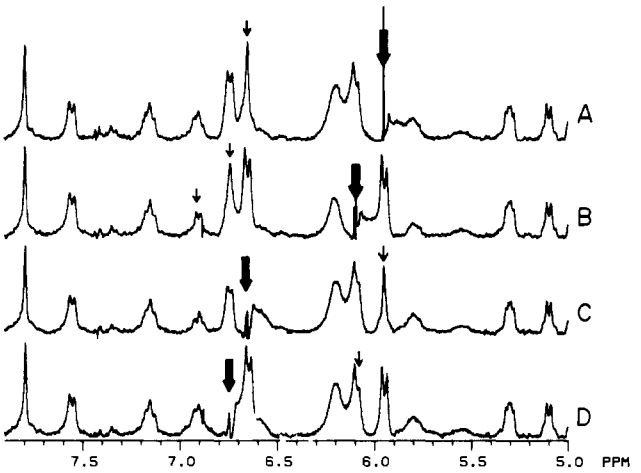

FIGURE 9: Aromatic region from 8 to 5 ppm in *Alcaligenes* ferrocytochrome *c*-554 at pH* 8, 40 °C, and decoupling patterns observed for aromatic protons. In the fully deuterium exchanged protein, no further peaks were observed downfield except for the meso protons shown in Figure 6. (A) Homonuclear irradiation of the doublet at 5.95 ppm (bold arrow) causes decoupling of the doublet at 6.65 ppm (small arrow). (B) Irradiation at 6.10 ppm causes decoupling of the doublet at 6.74 ppm and partial decoupling of the fine structure at 6.91 ppm. The reasons for the effect on two separate spin systems are discussed below. (C) Converse experiment to (A). Irradiation at 6.65 ppm decouples the doublet at 5.95 ppm. (D) Converse experiment to (B). Irradiation at 6.74 ppm causes a change in the fine structure at 6.10 ppm. While not readily apparent in the figure, the coupling constant of the doublet at 6.10 ppm was reproducibly observed to decrease by 0.9 Hz upon irradiation at 6.74 ppm. The peak at 6.10 ppm is interpreted as a superposition of a two-proton doublet from a tyrosine and a one-proton doublet from a tryptophan. Hence, irradiation of the coupled tyrosine doublet at 6.64 ppm causes only partial collapse of fine structure. This also explains why irradiation at 6.10 ppm also affects the tryptophan multiplet at 6.91 ppm in (B). The above pattern of decoupling supports the tyrosine assignments given in Table II.

amino acid composition of the protein, there are two tyrosines, one phenylalanine, one tryptophan, and one histidine (Timkovich et al., 1982). The sole histidine is the fifth ligand in cytochromes of the *c* type. The ring current of the heme is expected to shift ligand protons out of the normal aromatic region of the spectrum (Moore & Williams, 1980). Spin coupling patterns allow the assignment of spin systems to particular amino acid side chains (Moore & Williams, 1975). The decoupling experiments shown and described in Figure 9 establish the two doublets at 7.74 and 6.10 ppm as arising from the ring protons of one tyrosine, with the two doublets at 6.65 and 5.95 ppm arising from the other tyrosine. The apparent doublet at 5.95 ppm is the superposition of two doublets with slightly different coupling constants. These were resolved in the decoupling experiments described below.

Homonuclear spin decoupling experiments established that the doublet at 7.75 ppm was coupled to the triplet at 7.15 ppm, the triplet at 7.15 ppm was coupled to the doublet at 7.55 ppm as well as to the triplet at 6.91 ppm, and the triplet at 6.91 ppm was coupled to the triplet at 7.15 ppm and an unresolved doublet at circa 5.95 ppm. The mutual coupling is most evident in the *J*-modulated spin-echo experiment shown in Figure 10. The only amino acid side chain that would demonstrate this coupling pattern is tryptophan, and hence these peaks are assigned to the only tryptophan in the protein. Since ligand histidine resonances are not expected in this region, the singlet at 7.79 ppm is assigned to the C2 of the only tryptophan.

The obvious triplet at 5.30 ppm and the doublet at 5.10 ppm were not coupled to each other nor to any other spin system in the aromatic region. They may represent nonaromatic

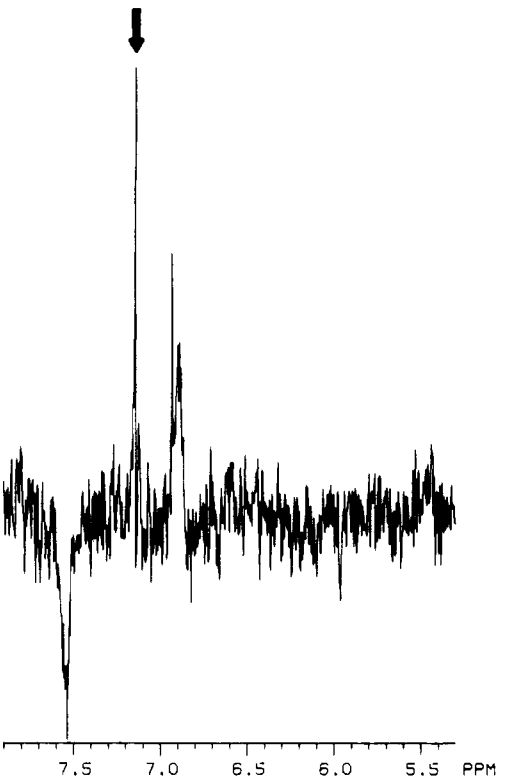

FIGURE 10: Assignment of the tryptophan resonances in *Alcaligenes* ferrocytochrome *c*-554 by *J*-modulated spin-echo difference spectroscopy. The difference spectrum shown is between a *J*-modulated spin-echo spectrum with τ = 64 ms and an equivalent spectrum in which the triplet at 7.15 ppm was irradiated. The negative peak shows that the 7.15 ppm triplet is coupled to a doublet at 7.55 ppm, and the positive peak shows coupling to another triplet at 6.91 ppm.

protons accidentally shifted into this region. Narrow resonances for the only phenylalanine residue have not been observed in the spectrum. This could well be a case where hindered rotation of the phenylalanine ring broadens the spin systems (Moore & Williams, 1975, 1980). The completed assignments have not accounted for all the area in the aromatic region. Unaccounted area remains at 6.6, 6.1, and 5.55 ppm; this could represent very broad, unresolved phenylalanine protons. Assignments for ferrocytochrome *c*-554 are summarized in Table II.

Discussion

For *Alcaligenes* cytochrome *c*-554, the assignments and interpretations that have been given rely upon analogy with other cytochromes that have been studied by ^{1}H NMR. This is not conclusive or definitive, but the evidence will become stronger as more cytochromes are studied by NMR techniques. The data from *Alcaligenes c*-554 certainly contribute to the expanding repertoire. For the ferrous cytochrome *c*-554, the known structures of other cytochromes, the distance dependence of the nuclear Overhauser effect, and the observation of spin-coupling patterns lend support to interpretations. For the ferric cytochrome, interpretations are most reliable where there is high homology to other cases. The assignment of resonances a, b, c, and d to heme methyls fits the general pattern discerned for cytochromes, in spite of the abnormal downfield shifts to greater than 40 ppm. The interpretation of pH effects on spectra fits repeated observations made on other cytochromes as well as the data in hand. Data interpretations are tentative in those instances where there is little analogy to other cytochromes, for example, in the cases of the temperature behavior of hyperfine-shifted resonances, the absence of an upfield methionyl methyl resonance in the ferric

spectrum, and the new presence of a three-proton resonance (e) in the downfield region. But these are precisely the most interesting aspects as they contribute new features. Therefore, some hypotheses should be offered.

The temperature dependence of the ferric *c*-554 spectrum is unique compared to previously studied cytochromes *c*. In other cytochromes *c*, some resonances move downfield with increasing temperature [for example, see Smith (1979)]. In *c*-554, all observed, resolved downfield hyperfine-shifted resonances except one (k) violate the usual temperature behavior. Four mechanisms are known to us that could in principle account for the anomalous temperature behavior. There could be a temperature-dependent reorientation of spin systems with respect to the electronic *g* tensor. An example is the case of heme vinyl groups (La Mar et al., 1978). This mechanism would affect only the pseudocontact contributions toward the total hyperfine shift. There could be a temperature-dependent reorientation of the electronic *g* tensor itself. This could be a localized phenomenon involving the iron inner coordination sphere or a shift of the entire heme plane within the heme crevice, while side chains remain reasonably fixed. This would affect predominantly the pseudocontact contributions. There could be a temperature dependence on the hyperfine (scalar) coupling constant. This would affect only those resonance shifts with an appreciable contact interaction component. It should be limited to directly bonded heme and axial ligand protons. There could be a temperature-dependent equilibrium between a small fraction of molecules in a high-spin state and a predominant fraction in a low-spin state, with increasing temperature favoring the high-spin state. The rate of interconversion must be fast compared to the NMR time scale, because only one set of resonances was observed at shifts more toward the range of low-spin ferric proteins. Although high-spin ferric proteins demonstrate hyperfine-shifted resonances that obey Curie's law, their total downfield shift is considerably greater than in the low-spin case. A net increase in the high-spin fraction would move resonances more downfield in the averaged spectrum than the Curie's law effect applied to each individual spin state. The most downfield heme methyl may be around 39 ppm for the usual low-spin state (Keller et al., 1980) vs. 85 ppm for the high-spin state (Emptage et al., 1981). In the absence of a direct observation of the hypothetical high-spin state, quantitative calculation of the exchange rate cannot be made, but, with reasonable assumptions, it is possible to make a limiting estimate. Taking 38 ppm as the furthest downfield shift for a typical low-spin methyl and 80 ppm as a typical value for a high-spin heme methyl and applying the usual equations for a system with chemical exchange (Pople et al., 1959), one calculates that the exchange rate must be greater than 10^5 s^{-1}. This mechanism could affect both contact and pseudocontact contributions to the total hyperfine shift.

Several possible mechanisms exist that could explain the observed line broadening in the ferric spectrum with decreasing temperature. These include a dipolar interaction with the electron spin, hindered methyl group rotations, chemical exchange involving hypothetical high-spin and low-spin forms, or Curie spin modulation (Johnson et al., 1977). The present data do not justify even a speculation on the relative merits of these mechanisms for the *c*-554 case. Deconvolution of the various contributions would be a formidable experimental task. It would certainly require extensive data at multiple field strengths.

Previous proton NMR studies of ferricytochromes have observed the sixth ligand methionyl methyl resonance in the extreme upfield region of the spectrum. As one of the five closest methyl groups to the paramagnetic iron (the other four are heme ring methyls), this group is expected to show a large hyperfine shift, mainly due to the dipolar (pseudocontact) contribution. For example, in horse and related eukaryotic cytochromes, it is found at circa −23 ppm (Redfield & Gupta, 1971), in *Rhodospirillum rubrum* cytochrome c_2 at −15 ppm (Smith & Kamen, 1974), and in *Pseudomonas aeruginosa* cytochrome *c*-551 at −17.6 ppm (Chao et al., 1979). The upfield region of the *c*-554 spectrum shown in Figure 4 is conspicuously lacking in such a methyl resonance. The broad resonance designated p at −6.75 ppm integrates to one proton. Yet visible spectroscopy and the ferrocytochrome proton NMR spectrum have indicated that methionine is the sixth ligand.

The question of the missing methyl resonance in the upfield region may be related to the appearance of an extra methyl resonance, labeled e in Figure 1, in the extreme downfield region. The peak width, large hyperfine shift, and temperature sensitivity of this resonance are all consistent with it being one of the closest spin systems to the heme iron. This resonance disappears in the cyano complex of *c*-554, but so do numerous other resonances observable in the native ferric form. Resonance e could arise from some amino acid side chain close to the heme iron in the structure of *c*-554. The thioether bridge methyls are not considered as candidates because they are fixed by covalent bonds relatively distant from the iron and previous assignments in other cytochromes have shown that their hyperfine shifts are much less than 25 ppm (Keller & Wutrich, 1978b). The assignment of resonance e to a non-methionine side chain would reflect a unique structure for *c*-554, because the crystal structures of homologous cytochromes do not show any side-chain methyl groups close enough to the iron to experience a pseudocontact shift as large as that observed for resonance e.

Another possibility is to assign resonance e to the ligand methionyl methyl. This assignment for ferricytochrome *c*-554 leads to a chemical shift difference of 50 ppm compared to its location in the spectrum of horse ferricytochrome *c*. While this is a staggering change, it could be feasible because of the strong interactions possible with paramagnetic iron. For a hyperfine shift due largely to the pseudocontact contribution, the shift depends upon the asymmetry of the electronic *g* tensor and the distance and orientation of the proton spin system with respect to the paramagnetic center [see eq 4 of LaMar & Walker-Jensen (1979) or eq 3.8 of Dwek (1973)]. The functional dependency is strong, depending upon differences of squared terms (*g* values or the orientation angle) or a term containing distance as an inverse third power. Therefore, subtle changes in the *g* tensor or changes in the iron–methionine bond could conceivably lead to major chemical shift differences. A previous hypothesis was given for the anomalous temperature behavior of the ferric spectrum in terms of a hypothetical high-spin state in equilibrium with a more usual low-spin state. A high-spin state could be produced by loss of the sixth ligand methionyl sulfur to iron bond. If so, then the methionyl methyl would spend some portion of its time in a conformation untypical of other cytochromes *c*. Averaging by chemical exchange could give rise to a drastically shifted methionyl methyl resonance. This hypothesis is by no means proven by the present data but is merely consistent with it. The highly unusual resonance e does suggest a novel structural feature in *Alcaligenes* *c*-554.

Previously studied ferricytochromes *c* show a distinctive pattern of hyperfine shifts for the four heme methyls in which resonances are grouped into two pairs with one pair further

downfield by at least 15 ppm than the other. The pattern has been shown to originate from asymmetry in the distribution of the unpaired electron spin of the ferric form into heme molecular orbitals (Redfield & Gutpa, 1971). In ferricytochrome *c*-554, there is some pairing of resonances a–b and c–d, but this is minimal compared to the overall large downfield shift of all heme methyls. The unpaired spin density distribution thus appears to be more symmetrical in *c*-554 than in other cytochromes. But there is high spin density on all heme pyrroles as evidenced by the large (40 ppm) shift of all methyls. *Alcaligenes c*-554 exhibits rapid electron-transport rates with bacterial cytochrome oxidase from *Alcaligenes* or from *Pseudomonas aeruginosa* (Timkovich et al., 1982). This could be argued two ways: either the asymmetric distribution is not kinetically significant for oxidation by a coupled oxidase or both oxidases react well with *c*-554 because *c*-554 can meet the symmetry requirements of both. A clear choice between alternatives is not possible at this time.

The absence of sharp resonances for the phenylalanine residue in ferrocytochrome *c*-554 suggests that this group may be subject to hindered rotation. It has not yet been possible to assign one tyrosine and one phenylalanine in *Pseudomonas c*-551 (Moore et al., 1977). Of the two phenylalanines observed in the crystal structure of *c*-551, only Phe-7 seems to be sufficiently well packed to have hindered rotation of the ring. Therefore, the hindered Phe in *Alcaligenes* may be the analogue of Phe-7 in *Pseudomonas c*-551.

The chemical shifts of the tryptophan group in *c*-554 are highly unusual in that they show large changes from the expected primary positions of resonances in the free amino acid and also from observed tryptophan shifts in many other cytochromes. The usual pattern for fine structure is doublet (C4 or C7), doublet (C7 or C4), singlet (C2), triplet (C5 or C6), and triplet (C6 or C5), with the most downfield spin system given first. The observed pattern in *c*-554 is singlet, doublet, triplet, triplet, doublet. The far downfield shift of the tryptophan singlet (C2) is also observed for one of two tryptophan residues in *Pseudomonas c*-551 (Moore et al., 1977). Examination of the crystal structure for *c*-551 (Almassy & Dickerson, 1978) reveals that the conserved residue Trp-56 hydrogen bonds to a heme propionate and is oriented so that the proton attached to C2 is directed near to the heme edge. This proton would thus experience a ring current, shifting the resonance downfield. The C7 benzenoid proton of Trp-56 is oriented approximately above the ring plane of a nearby aromatic proton at position 34. In *c*-551, a possible ring current with this group is apparently not large, because the doublets observed in *c*-551 are in the usual pattern. In *c*-554, a minor structural repacking could bring a ring current close to the doublet spin system of C7 and account for the upfield shift observed in *c*-554. Another highly conserved tryptophan residue is located near the carboxyl terminus in *c*-551 and in small photosynthetic cytochromes (Ulrich et al., 1982). There is, however, no obvious mechanism in this locale to account for the chemical shifts observed for *Alcaligenes c*-554. By the above arguments, it is concluded that the sole tryptophan in *c*-554 is the analogue of Trp-56 in *c*-551.

Acknowledgments

Technical assistance was provided by Priscilla Taylor.

Registry No. Cytochrome *c*-554, 52932-67-9.

References

Almassy, R. J., & Dickerson, R. E. (1978) *Proc. Natl. Acad. Sci. U.S.A. 75*, 2674–2678.

Campbell, I. D., & Dobson, C. M. (1975) *J. Chem. Soc., Chem. Commun.*, 750–751.

Chao, Y. H., Bersohn, R., & Aisen, P. (1979) *Biochemistry 18*, 774–779.

Dickerson, R. E., & Timkovich, R (1975) *Enzymes, 3rd Ed. 11*, 395–544.

Dickerson, R. E., Timkovich, R., & Almassy, R. J. (1976) *J. Mol. Biol. 100*, 473–491.

Dubs, A., Wagner, G., & Wuthrich, K. (1979) *Biochim. Biophys. Acta 577*, 177–194.

Dwek, R. A. (1973) *NMR in Biochemistry*, pp 174–212, Clarendon Press, Oxford, England.

Emptage, M. H., Xavier, A. V., Wood, J. M., Alsaadi, B. M., Moore, G. R., Pitt, R. C., Williams, R. J. P., Ambler, R. P., & Bartsch, R. G. (1981) *Biochemistry 20*, 58–64.

Freeman, R., Kempsell, S. P., & Levitt, M. H. (1980) *J. Magn. Reson. 38*, 453–479.

Gupta, R. K., & Redfield, A. G. (1970) *Biochem. Biophys. Res. Commun. 41*, 273–281.

IUPAC–IUB Commission on Biochemical Nomenclature (1975) *Biochemistry 14*, 499–462.

Johnson, M. E., Fung, L. W. M., & Ho, C. (1977) *J. Am. Chem. Soc. 99*, 1245–1250.

Keller, R., Groudinsky, O., & Wuthrich, K. (1976) *Biochim. Biophys. Acta 427*, 497–511.

Keller, R. M., & Wuthrich, K. (1978a) *Biochem. Biophys. Res. Commun. 83*, 1132–1139.

Keller, R. M., & Wuthrich, K. (1978b) *Biochim. Biophys. Acta 533*, 195–208.

Keller, R. M., Wuthrich, K., & Pecht, I. (1976) *FEBS Lett. 70*, 180–184.

Keller, R. M., Schejter, A., & Wuthrich, K. (1980) *Biochim. Biophys. Acta 626*, 15–22.

La Mar, G. N., & Walker-Jensen, F. A. (1979) in *The Porphyrins* (Dolphin, D., Ed.) Vol. IVB, pp 61–159, Academic Press, New York.

La Mar, G. N., Viscio, D. B., Gersonde, K., & Sick, H. (1978) *Biochemistry 17*, 361–367.

McLaughlin, A. C., & Leigh, J. S., Jr. (1973) *J. Magn. Reson. 9*, 296–304.

Moore, G. R., & Williams, R. J. P. (1975) *FEBS Lett. 53*, 334–338.

Moore, G. R., & Williams, R. J. P. (1980) *Eur. J. Biochem. 103*, 493–502.

Moore, G. R., Pitt, R. C., & Williams, R. J. P. (1977) *Eur. J. Biochem. 77*, 53–60.

Moore, G. R., Pettigrew, G. W., Pitt, R. C., & Williams, R. J. P. (1980) *Biochim. Biophys. Acta 590*, 261–271.

Pople, J. A., Schneider, W. G., & Bernstein, H. J. (1959) *High Resolution NMR*, pp 218–224, McGraw-Hill, New York.

Redfield, A. G., & Gupta, R. K. (1971) *Cold Spring Harbor Symp. Quant. Biol. 36*, 405–411.

Senn, H., Keller, R. M., & Wuthrich, K. (1980) *Biochem. Biophys. Res. Commun. 92*, 1362–1369.

Shulman, R. G., Glarum, S. H., & Karplus, M. (1971) *J. Mol. Biol. 57*, 93–115.

Smith, G. M. (1979) *Biochemistry 18*, 1628–1634.

Smith, G. M., & Kamen, M. D. (1974) *Proc. Natl. Acad. Sci. U.S.A. 71*, 4303–4306.

Timkovich, R. (1980) *Biochem. J. 185*, 47–57.

Timkovich, R., & Cork, M. S. (1982) *Biochemistry 21*, 5119-5123.
Timkovich, R., Dhesi, R., Martinkus, K., Robinson, M. J., & Rea, T. M. (1982) *Arch. Biochem. Biophys. 215*, 47-58.
Ulrich, E. L., Krogmann, D. W., & Markley, J. L. (1982) *J. Biol. Chem. 257*, 9356-9364.
Wuthrich, K. (1969) *Proc. Natl. Acad. Sci. U.S.A. 63*, 1071-1078.

Stoichiometry and Specificity of Lipid-Protein Interaction with Myelin Proteolipid Protein Studied by Spin-Label Electron Spin Resonance†

Peter J. Brophy,‡ László I. Horváth,§ and Derek Marsh*

ABSTRACT: The interaction of spin-labeled lipids with the myelin proteolipid apoprotein in complexes with dimyristoylphosphatidylcholine of varying lipid/protein ratios has been studied with electron spin resonance spectroscopy. A first shell of approximately 10 lipids per 25000-dalton protein is found to be motionally restricted by the protein interface. This stoichiometry is consistent with a hexameric arrangement of the protein in the membrane. A selectivity of the various spin-labeled lipids for the motionally restricted component at the protein interface is found in the order stearic acid > phosphatidic acid > cardiolipin ≳ phosphatidylserine > phosphatidylglycerol ≈ phosphatidylcholine > phosphatidylethanolamine > androstanol ≳ cholestane.

Interactions between lipids and proteins in biological membranes can exert a major influence on membrane protein function (Sanderman, 1978). It is therefore of considerable interest to determine the stoichiometry of the lipid-protein interactions and whether particular membrane proteins display any specificity in their interactions with lipids. Jost et al. (1973) were the first to demonstrate the existence of motionally restricted lipid in the immediate environment of an integral membrane protein using electron spin resonance (ESR)[1] spectroscopy. From the stoichiometry of the interaction, the lipid that they observed to be motionally restricted on the conventional ESR time scale was described as boundary lipid. Such motionally restricted lipid has subsequently been demonstrated in other systems, including rod outer segment disk membranes (Watts et al., 1979, 1981), acetylcholine receptor membranes (March & Barrantes, 1978; Marsh et al., 1981), and Na,K-ATPase membranes (Brotherus et al., 1980; Marsh et al., 1982). Boundary lipid would be expected to be enriched in any lipids for which a membrane protein showed a preferential interaction, and this has been demonstrated in certain cases (Brotherus et al., 1980; Knowles et al., 1981; Marsh et al., 1982). Because of its characteristic time scale, ESR spectroscopy is therefore an attractive technique for identifying and quantifying the lipids that interact with membrane proteins [see Marsh & Watts (1982) for a review].

The proteolipid protein is the major integral membrane protein of central nervous system myelin. The same protein isolated from human myelin has been called lipophilin (Moscarello, 1976). The proteolipid protein can be readily purified and recombined with defined lipids, and this has made the protein a suitable subject for studying the interactions of lipids with an integral membrane protein [see Boggs et al. (1982) for a review]. The existence of motionally restricted lipid in lipophilin-egg phosphatidylcholine complexes has been demonstrated by the use of spin-labeled fatty acids (Boggs et al., 1976). Boggs and co-workers have investigated the nature of the lipid-lipophilin interactions further by calorimetric techniques. They have shown that the protein preferentially associates with negatively charged phospholipids (Boggs et al., 1977) and that these interactions are independent of fatty acid chain length between C-14 and C-18 (Boggs & Moscarello, 1978). In three different calorimetric studies the number of lipid molecules removed from the cooperative calorimetric transition has variously been estimated as 15, 21-25, and 20-35 per 25000-dalton protein (Papahadjopoulos et al., 1975; Boggs & Moscarello, 1978; Boggs et al., 1980).

Since the proteolipid apoprotein is considerably more hydrophobic in character than the amphipathic integral membrane proteins that we have studied previously [see, e.g., Marsh et al. (1982) and Marsh & Watts (1982)], it is an attractive candidate for more detailed study. In this paper we have investigated phospholipid interactions with the proteolipid protein from bovine central nervous system myelin using ESR spectroscopy. The proteolipid protein has been reconstituted with dimyristoylphosphatidylcholine (DMPC) in the presence of a variety of spin-labeled phospholipids. In this way we have been able to investigate both the specificity and the stoichiometry of lipid interaction with the protein. An interesting pattern of lipid specificity emerges, and the relatively low lipid/protein stoichiometry suggests an oligomeric form for the protein in the membrane.

† From the Max-Planck-Institut für biophysikalische Chemie, Abteilung Spektroskopie, D-3400 Göttingen, Federal Republic of Germany. *Received July 26, 1983.* P.J.B. received a project grant from the Science and Engineering Research Council and a travel grant from the Federation of European Biochemical Societies.

‡ Permanent address: Department of Biological Science, Stirling University, Stirling FK9 4LA, U.K.
§ Permanent address: Institute of Biophysics, Biological Research Centre, Szeged, Hungary.

[1] Abbreviations: ESR, electron spin resonance; Hepes, *N*-(2-hydroxyethyl)piperazine-*N*'-2-ethanesulfonic acid; PLP, proteolipid apoprotein; DMPC, 1,2-dimyristoyl-*sn*-glycero-3-phosphocholine; 14-PCSL, -PESL, -PGSL, -PSSL, and -PASL, 1-acyl-2-[14-(4,4-dimethyloxazolidine-*N*-oxyl)stearoyl]-*sn*-glycero-3-phosphocholine, -phosphoethanolamine, -phosphoglycerol, -phosphoserine, and -phosphoric acid; 14-CLSL, 1-(3-*sn*-phosphatidyl)-3-[1-acyl-2-[14-(4,4-dimethyloxazolidine-*N*-oxyl)stearoyl]glycero-3-phospho]-*sn*-glycerol; 14-SASL, 14-(4,4-dimethyloxazolidine-*N*-oxyl)stearic acid; ASL, 17β-hydroxy-4',4'-dimethylspiro[15α-androstane-3,2'-oxazolidin]-3'-yloxy; CSL, 4',4'-dimethylspiro[5α-cholestane-3,2'-oxazolidin]-3'-yloxy. The stearoyl component of 14-PCSL etc. should more systematically be named 13-(2-butyl-4,4-dimethyl-3-oxyoxazolidin-2-yl)tridecanoyl.

0006-2960/84/0423-0860$01.50/0